

Research Article

Synthesis, Characterization, and Photocatalytic Activity of N-Doped ZnO/ZnS Composites

Hongchao Ma, Xiaohong Cheng, Chun Ma, Xiaoli Dong, Xinxin Zhang, Mang Xue, Xiufang Zhang, and Yinghuan Fu

School of Chemistry Engineering and Material, Dalian Polytechnic University, Dalian, Liaoning 116034, China

Correspondence should be addressed to Xiaoli Dong; dongxl@dlpu.edu.cn and Yinghuan Fu; fuyinghuan@sina.com

Received 19 November 2012; Accepted 31 December 2012

Academic Editor: Raghu N. Bhattacharya

Copyright © 2013 Hongchao Ma et al. This is an open access article distributed under the Creative Commons Attribution License, which permits unrestricted use, distribution, and reproduction in any medium, provided the original work is properly cited.

The aim of the present study is to enhance photocatalytic performance of ZnO semiconductor by comodification with doping of nonmetal ions and coupling with another semiconductor. Therefore, we synthesized the N-doped ZnO/ZnS photocatalysts via a simple heat-treatment approach using L-cysteine as N and S source in this work. Anthraquinone dye (reactive brilliant blue KNR) is employed as the model contaminants to evaluate the photocatalytic activity of as-synthesized samples under sunlight illumination. The N-doped ZnO/ZnS synthesized by this method shows better photocatalytic activity as compared to that of pure ZnO. The enhanced photocatalytic activity of the N-doped ZnO/ZnS composites may be related to the existence of N doping, ZnS/ZnO heterostructure, and covered abundant carbon species on the photocatalyst surface, which causing high absorption efficiency of light, efficient separation of electron-hole pairs, and quick surface reaction in doped ZnO.

1. Introduction

Semiconductor photocatalysis is an efficient approach for environmental decontamination by the chemical utilization of solar energy [1–4], which is capable of converting the toxic and nonbiodegradable organic compounds into carbon dioxide and inorganic constituents. Among the various semiconductors applied, TiO₂ is the most frequently employed photocatalyst owing to its cheapness, nontoxicity, and structural stability [5–8]. Currently, researchers show that ZnO has better activity in photocatalytic degradation of some organic contaminants compared to that of TiO₂ [9–11]. However, ZnO semiconductor has a wide band gap of about 3.37 eV, which results in that it is effective only under irradiation of UV-light region and suffers from low efficiency under visible light illumination. Thus, only approximately 3%–5% UV light of the solar energy that reaches the earth can be utilized for photocatalytic reactions when ZnO is used as the catalyst. Furthermore, the fast recombination of photogenerated electron-hole pairs also needs to be solved for its application [12]. Therefore, improving photocatalytic performance of ZnO by modification to reduce the band gap to make absorption in the visible region possible (use sunlight

more efficiently) and to inhibit recombination of photo-generated electron-hole pairs has become a hot topic among researchers in recent years [13, 14].

Numerous efforts have been developed to overcome the drawbacks, such as depositing metals on ZnO surface [15, 16], doping with metals (Co²⁺, Mg²⁺) or nonmetal ions (C, S, N) [14, 17–19], or combining ZnO with another semiconductor [20, 21]. Recently, nonmetal ions doped ZnO photocatalysts have attracted much attention in the photo-catalytic processes owing to that it can improve photocatalytic activity by enhancing absorption of light and transport of photo-generated charge carriers [19, 22]. However, to the best of our knowledge, previous researches mostly regarded onefold modification of ZnO with non metal ions such as C, N, S co-doped ZnO or C, N codoped ZnS photocatalysts [14, 23]; few studies have been done on comodification with doping of nonmetal ions and coupling with another semiconductor to enhance photocatalytic performance of semiconductor. Therefore, in the present work, we synthesized the N-doped ZnO/ZnS photocatalysts with visible-light response via a simple heat-treatment approach using L-cysteine as N and S source. Anthraquinone dye (reactive brilliant blue KN-R)

is employed as the model contaminants to evaluate the photocatalytic activity of as-synthesized samples under sunlight illumination. The N-doped ZnO/ZnS synthesized by this method shows better photocatalytic activity as compared to that of pure ZnO.

2. Experimental Details

2.1. Synthesis. 2.875 g $\text{ZnSO}_4 \cdot 7\text{H}_2\text{O}$ (0.01 mol), 0.8 g NaOH (0.02 mol), and desired amount of L-cysteine (the molar ratio of Zn to L-cysteine is 10:1, 5:1, 1:1, and 1:5) were dissolved in 40 mL deionized water. After 10 min of stirring, the reaction mixture was evaporated on water bath at 90°C until dry mixture was obtained, followed by transferring into an annealing furnace and maintained at 300, 400, 500, and 600°C for 2 h in nitrogen atmosphere. After calcination, the powder was collected, washed with deionized water and anhydrous alcohol for three times, and dried at 80°C for 6 h to obtain N-doped ZnO/ZnS composites. For comparison, pure ZnO was prepared by the same process with synthesis of N, S co-doped ZnO composite in absence of L-cysteine and calcined at 400°C 2 h in this process.

2.2. Characterizations. The products were characterized by X-ray powder diffraction on a Shimadzu XRD-6100 X-ray diffractometer with a graphite monochromatized CuK α radiation ($\lambda = 1.5418 \text{ \AA}$). UV-visible diffuse reflectance spectra were recorded with a Varian Cary-100 spectrophotometer and barium sulfate was used as a standard. The surface structure of the as-prepared sample was determined by X-ray photoelectron spectroscopy (XPS) and was performed using VG EscaLab 250 SYSTEM (Thermo VG) with Al K α radiation (1486.6 eV). The Cls photoelectron peak (binding energy at 284.6 eV) was used as energy reference. The PL spectra of ZnO microcrystal photocatalyst were measured by using a fluorescence spectrophotometer (PE-LS55, USA) equipped with a Xenon lamp at an excitation wavelength of 325 nm.

2.3. Photocatalytic Activity Test. The photocatalytic activities of the samples were evaluated by the degradation of anthraquinone dye (reactive brilliant blue KN-R) in an aqueous solution. 200 mL anthraquinone dye aqueous solution with concentration of 20 mg/L was mixed with 20 mg/L catalysts, which was exposed to illumination of 500 W Xe lamp (as simulated sunlight source) with a maximum emission at about 470 nm. Before turning on the lamp, the suspension containing reactive brilliant blue KN-R and photocatalyst were magnetically stirred in a dark condition for 60 min till an adsorption-desorption equilibrium was established. Samples were then taken out regularly from the reactor and centrifuged immediately for separation of any suspended solid. The absorbance A of transparent solution was measured by a 721B spectrophotometer and the A value was used to estimate the photocatalytic degradation rate D of reactive brilliant blue K-NR according to the following equation:

$$D = \frac{(A_0 - A_t)}{A_0} \times 100\%, \quad (1)$$

where A_0 is the initial absorbance of reactive brilliant blue K-NR, t is the reaction time, and A_t is the absorbance at time t .

3. Results and Discussion

Figure 1(a) shows the XRD patterns of the N-doped ZnO/ZnS samples calcined at various temperatures. The main diffraction peaks can be indexed for hexagonal wurtzite ZnO (JCPDS card no. 36-1451) and sphalerite cubic ZnS phase (JCPDS card no. 5-0566) in XRD pattern of powders obtained by calcination at $300\text{--}500^\circ\text{C}$. When the calcination temperature of as-synthesized sample reached 600°C , the characteristic peaks of wurtzite ZnS phase is found, while all the characteristic peaks of sphalerite cubic ZnS disappeared. The XRD pattern of as-synthesized samples with different Zn/N molar ratios is shown in Figure 1(b). It can be seen from Figure 1(b) that intensity of diffraction peaks corresponding to ZnO increases with increasing of Zn/N atomic ratio, while intensity of diffraction peaks corresponding to ZnS decreases. The XRD patterns of the (100), (002), and (101) planes of the samples were shown in Figure 1(c). The peaks of these planes in N-doped ZnO/ZnS samples shift slightly to lower Bragg angle (by 0.07°) as compared to those of pure ZnO. This shift suggests that the oxygen or Zn atoms in the lattice of doped ZnO samples may be substituted by other atoms. We consider that the position of diffraction peaks in doped samples shifts to lower Bragg angle, which may be contributed to the fact that atomic radius of N is greater than O and smaller than Zn; it is suggested that N is substituted on O sites [24].

The optical properties of the as-synthesized samples were probed by UV-visible diffuse reflectance spectroscopy. Figure 2 shows the transformed UV-vis absorption spectra of the as-synthesized samples together with the band-gap values, evaluated by linear extrapolation (the intercept on the x -axis gives the value of the band gap). The spectrum of pure ZnO is also included for comparison. From Figure 2, it is clear that N-doped ZnO/ZnS samples show obvious red shift as compared to those of pure ZnO. It is found that the band-gap of N-doped ZnO/ZnS samples decreases with the increasing of the Zn/N molar ratios. Oppositely, the change of band gap with heat treating is irregular, which suggests that the effect of heat treating on structure of photocatalysts may be more complex. Nevertheless, a minimum value of band gap (2.98 eV) can be observed in N-doped ZnO/ZnS sample with Zn/N = 1 prepared by calcination at 400°C . The red shift of the band-gap absorption edge for N-doped ZnO/ZnS can be associated with the formed impurity states in the band gap by the partial substitution of O with other atoms in the crystal lattice of ZnO [22]. Thus, the N-doped ZnO/ZnS can be used as an efficient photocatalyst under sunlight irradiation.

The PL spectrum of the samples was measured by an excitation wavelength of 325 nm at room temperature and shown in Figure 3. The PL peak at about 390–400 nm was observed for doped ZnO and pure ZnO. The PL peak can be contributed to the recombination of photo-generated electrons and holes [25, 26]. It can be seen that from Figure 3 the N-doped ZnO/ZnS composites showed lower intensity of PL peak located at 390–400 nm than that of pure ZnO, especially the composite with 1:1 of Zn/N atomic ratio showed lowest PL intensity. The PL spectra indicate that the effect of doped impurities on the recombination of photo-generated charges depended on the content of impurities.

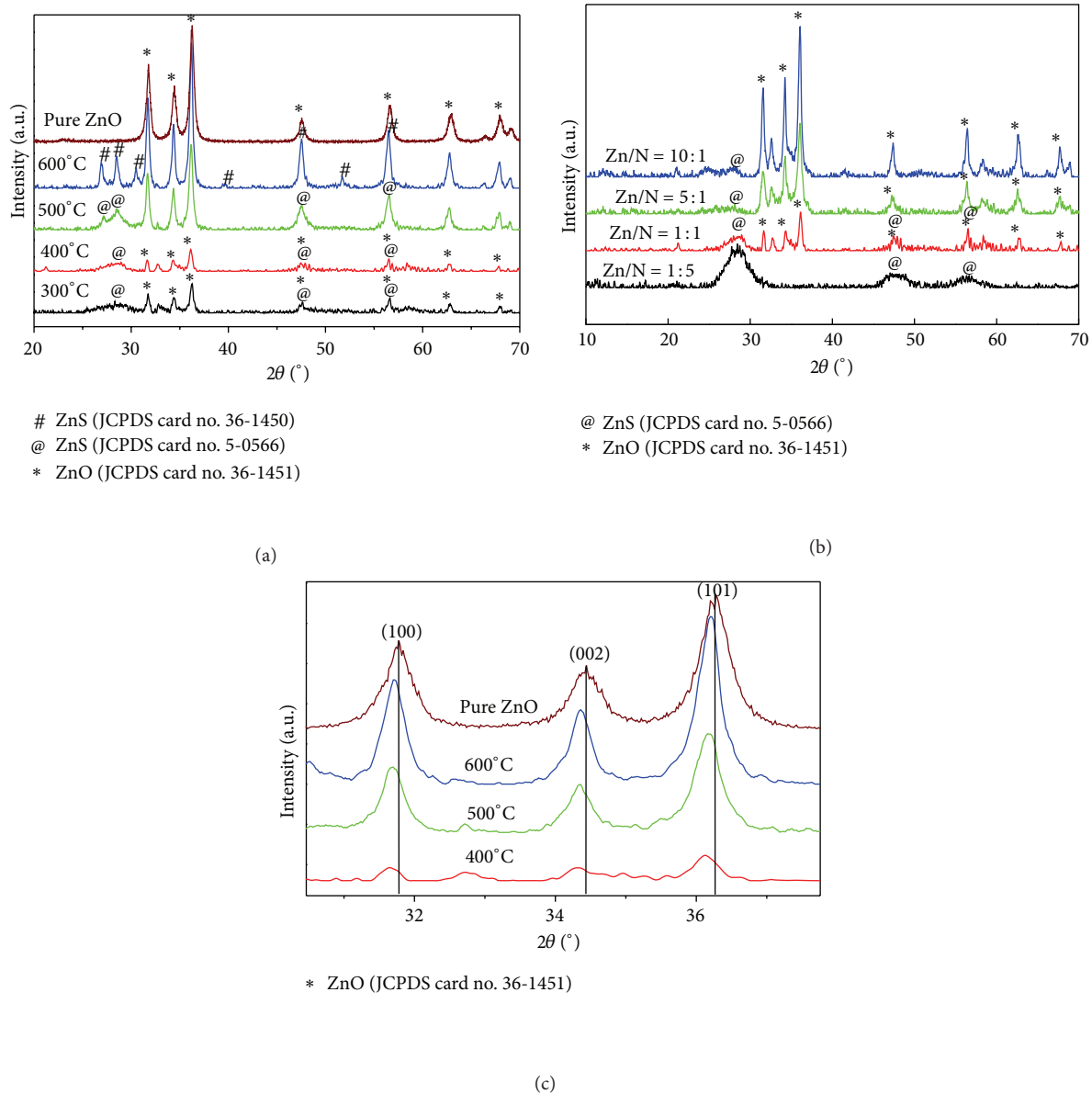


FIGURE 1: XRD patterns of as-synthesized samples: (a) samples with Zn/N = 1:1 molar ratios calcined at different temperatures, (b) samples with different Zn/N molar ratios calcined at 400°C, and (c) comparison for peaks position between N-doped ZnO/ZnS composites and pure ZnO.

The excessive impurities would form recombination center of photo-generated charges, which improved their recombination. The PL results demonstrated that impurity doping can inhibit the recombination between photogenerated holes and electrons, which is beneficial for the photocatalytic reaction.

The surface composition and chemical state of as-synthesized samples were determined by XPS analysis. Figure 4(a) shows the whole scanning spectrum of as-synthesized samples. The stronger signals of S2p, Cls and a weak signal corresponding to N1s were observed in doped ZnO sample as compared to those of pure ZnO, which indicates S, N, and C elements exist in doped ZnO sample. The Cls XPS spectrum of doped ZnO was fitted to three peaks at 284.5, 286.5 eV, and 288.3 eV (see Figure 4(b)). The peak with

a binding energy of 284.5 eV can be assigned to adventitious carbon adsorbed on the surface of the sample [27]. The other two peaks at 286.5 and 288.3 eV can be assigned to the existence of Zn–O–C and C=O of carbonate species, respectively [28, 29]. The peak around 282 eV resulting from carbon interacting with Zn through Zn–C bond formation was not observed [30], which suggests that new chemical state of carbon species (Zn–C) is not formed during the doping process. Even so, the existence of abundant carbon species on the surface of composite still is beneficial for photocatalytic process because it can set in contact with external pollutant molecules.

Figure 4(c) shows the high resolution XPS spectra of N1s region for doped ZnO sample and its fitting curves. It can be

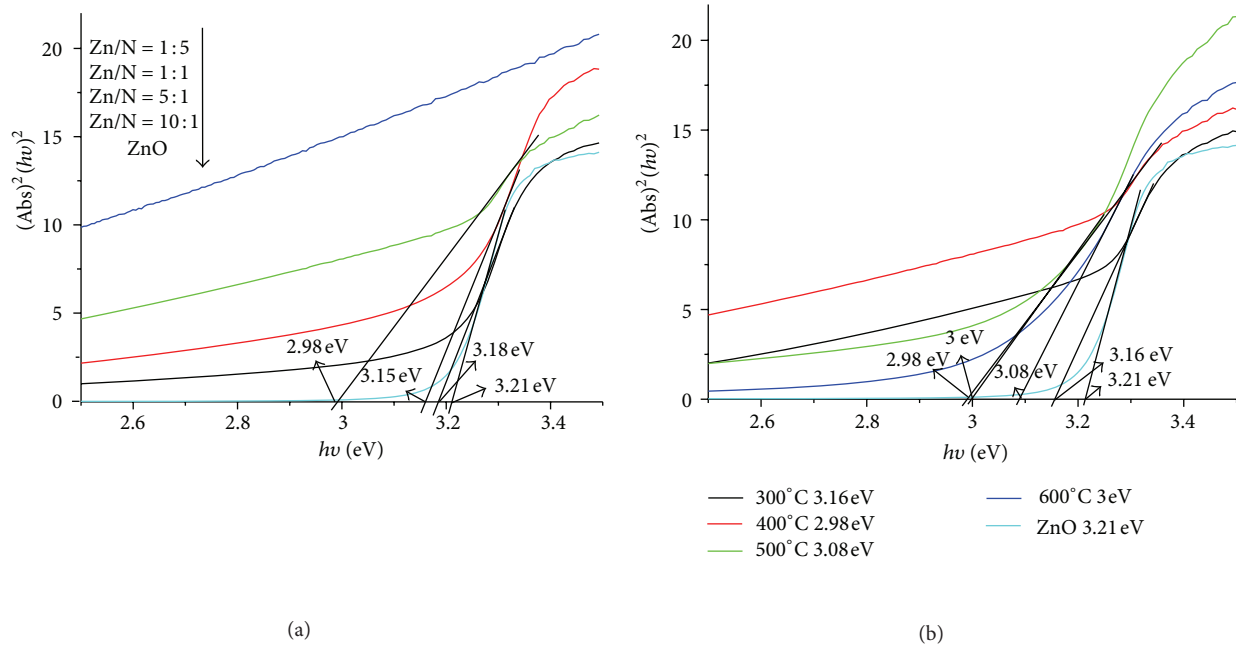


FIGURE 2: UV-vis absorption spectra in the band-gap region of samples: (a) samples with different Zn/N molar ratios calcined at; 400°C; (b) samples with Zn/N = 1 : 1 molar ratios calcined at different temperatures.

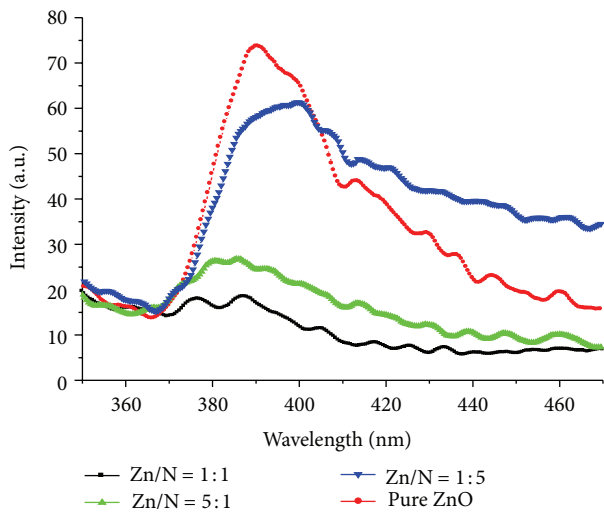


FIGURE 3: Photoluminescence spectra of samples with different Zn/N molar ratios calcined at 400°C.

seen that a peak centered at 398.8 eV for the doped sample is obtained, which can be ascribed to the anionic N^- in the form of N-Zn bonds [31–34]. Thus the XPS data supports the incorporation of N into the ZnO. The substitutional N may be related to the active sites for the photocatalysts [35]. The high resolution XPS spectrum of the S2p region of doped ZnO sample is shown in Figure 4(d). It can be seen that the peak of S2p contains two isolated bands centered at 169.2 and 161.8 eV, which can be attributed to the S^{4+}/S^{6+} and S^{2-} according to the data reported in the literature [28, 36–39]. Thus, based on mentioned XRD, UV-vis, and XPS analysis it can be

reasonable to deduce that the N-doped ZnO/ZnS composite was successfully synthesized by simple heat-treated process.

The high resolution XPS spectra of O1s band of as-synthesized samples are shown in Figure 4(e). The O1s peak was fitted to two components centered at about 529.8–530.5 eV and 531.5–532.0 eV, respectively. The low binding energy component at 529.8–530.5 eV was attributed to O^{2-} ions of ZnO [40], while another at 531.5–532.0 eV usually corresponds to oxygen in adsorbed O_2 or OH^- groups on the ZnO surface [41–43]. In this study, it is considered that some S, C, and N atoms may bound to oxygen in the sample; the peak at 531.5–532.0 eV may also be assigned to O bound to S, N, or C atom [14]. In addition, from the high resolution XPS spectra of $Zn2p_{3/2}$ (Figure 4(f)), it can be seen that the $Zn2p_{3/2}$ peaks of pure ZnO and doped ZnO appears at 1020.8 and 1023.6 eV, respectively. It is clear that the binding energy of $Zn2p_{3/2}$ peak of doped ZnO is higher as compared to that of the pure ZnO. The shift of $Zn2p_{3/2}$ peak for doped ZnO can be ascribed to the doping or incorporation of N ions into ZnO powders and the existence of Zn-S bond structure [44, 45].

The photocatalytic evaluation of as-synthesized samples is carried out for degradation of reactive brilliant blue KN-R. The straight lines for all reactions were obtained when $\ln(C_0/C_t)$ was plotted against time (see Figure 5), which indicated that the photodegradation process corresponds well to pseudofirst-order kinetics. It can be seen that the N-doped ZnO/ZnS composites exhibited higher photodegradation rate than the pure ZnO. The improvement of photocatalytic activity for N-doped ZnO/ZnS should be related to the nitrogen doping, ZnS/ZnO hetero-structure, and covered carbon species on the photocatalyst surface, which causing high absorption efficiency of light, efficient separation of electron-hole pairs, and quick surface reaction

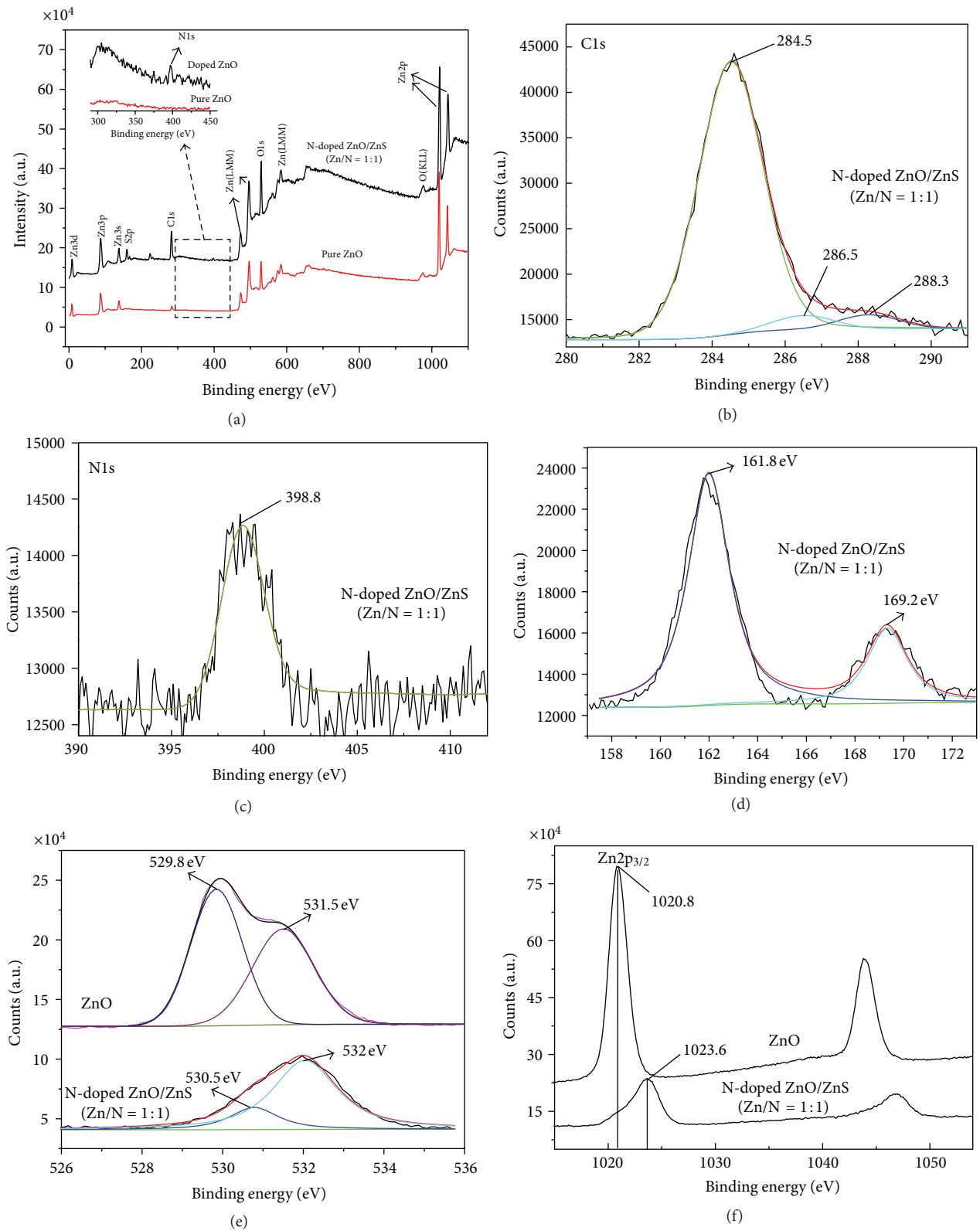
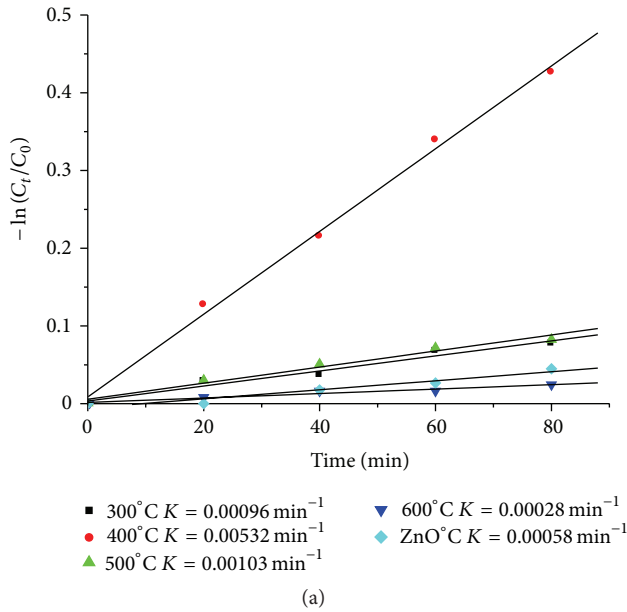
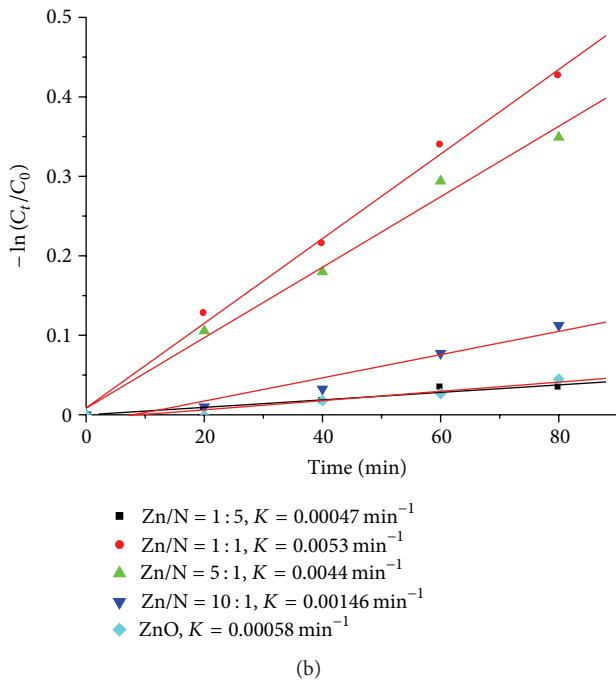


FIGURE 4: XPS spectra of samples: (a) XPS survey spectra, (b) C1s, (c) N1s, (d) S2p, (e) O1s, and (f) Zn2p state.



(a)



(b)

FIGURE 5: Plots of degradation of KN-R over as-synthesized samples under visible light irradiation; (a) N-doped ZnO/ZnS photocatalysts with Zn/N = 1 prepared at different temperatures for 2 h. (b) N-doped ZnO/ZnS photocatalysts with various Zn/N ratios prepared at 400°C for 2 h.

in doped ZnO. The N-doped ZnO/ZnS composite obtained under optimum conditions (Zn/N = 1:1 and heat treated at 400°C for 2 h) has a highest degradation rate, and the apparent rate constant k was 0.0053 min⁻¹. The photodegradation rate of the N-doped ZnO/ZnS composite prepared at optimum conditions is about 9.1 times more than that of pure ZnO for reactive brilliant blue KN-R degradation under sunlight irradiation. It is well known that the stability of the ZnO is an important concern for the repeated use of the

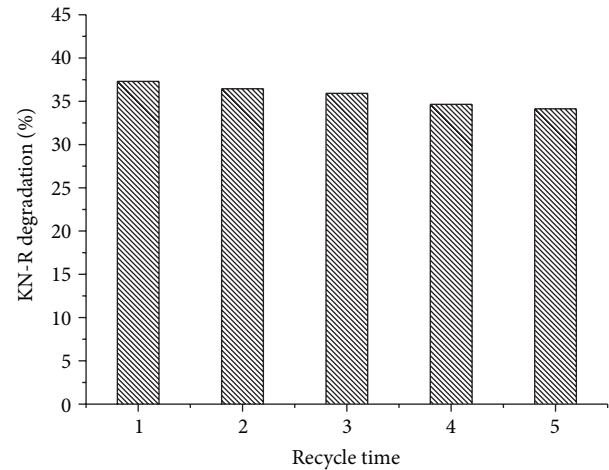


FIGURE 6: The photocatalytic cycling tests of N-doped ZnO/ZnS composite obtained under optimum conditions (Zn/N = 1:1 and heat treated at 400°C for 2 h).

photocatalysts, so the photodegradative cycling experiments were carried out under sunlight irradiation, and each run lasted 120 min (see Figure 6). The results in Figure 6 show that the photocatalytic activity of N-doped ZnO/ZnS composite does not exhibit any great loss in activity even after five times, which implied that the stability of N-doped ZnO/ZnS composite is suitable for the photodegradation process of pollutants.

4. Conclusions

In this work, the N-doped ZnO/ZnS composites were synthesized by simple heat-treating method using L-cysteine as N and S source. The XRD, XPS, UV-vis DRS, and PL studies showed that the N is incorporated to ZnO/ZnS composites, which shifted the band-gap absorption edge to visible light region and inhibited recombination of photogenerated electron-hole pairs. Hence, the as-synthesized N-doped ZnO/ZnS composites show better photodegradation rate of reactive brilliant blue KN-R as compared to that of pure ZnO under sunlight irradiation. The photo-degradation rate of N-doped ZnO/ZnS composite prepared under optimum conditions (Zn/N = 1:1 and heat treated at 400°C for 2 h) was found to be 9.1-times greater than that of pure ZnO.

Acknowledgments

This work was supported by the National Natural Science Foundation of China (21243005), Science and Technology Foundation of Liaoning of China (201102111), Program for Key Science and Technology Platform in Universities of Liaoning Province, Program for Liaoning Excellent Talents in University (LGQ-2011-054, LR2011011), and Science & Technology Public-Benefit Foundation of Liaoning of China ([2011]49).

References

- [1] N. Sobana and M. Swaminathan, "The effect of operational parameters on the photocatalytic degradation of acid red 18 by ZnO," *Separation and Purification Technology*, vol. 56, no. 1, pp. 101–107, 2007.
- [2] M. Mrowetz and E. Selli, "Photocatalytic degradation of formic and benzoic acids and hydrogen peroxide evolution in TiO₂ and ZnO water suspensions," *Journal of Photochemistry and Photobiology A*, vol. 180, no. 1-2, pp. 15–22, 2006.
- [3] K. Chiang, T. M. Lim, L. Tsen, and C. C. Lee, "Photocatalytic degradation and mineralization of bisphenol A by TiO₂ and platinumized TiO₂," *Applied Catalysis A*, vol. 261, no. 2, pp. 225–237, 2004.
- [4] H. Lachheb, E. Puzenat, A. Houas et al., "Photocatalytic degradation of various types of dyes (Alizarin S, Crocein Orange G, Methyl Red, Congo Red, Methylene Blue) in water by UV-irradiated titania," *Applied Catalysis B*, vol. 39, no. 1, pp. 75–90, 2002.
- [5] A. L. Linsebigler, G. Lu, and J. T. Yates, "Photocatalysis on TiO₂ surfaces: principles, mechanisms, and selected results," *Chemical Reviews*, vol. 95, no. 3, pp. 735–758, 1995.
- [6] A. Fujishima, T. N. Rao, and D. A. Tryk, "Titanium dioxide photocatalysis," *Journal of Photochemistry and Photobiology C*, vol. 1, no. 1, pp. 1–21, 2000.
- [7] S. Klosek and D. Raftery, "Visible light driven V-doped TiO₂ photocatalyst and its photooxidation of ethanol," *Journal of Physical Chemistry B*, vol. 105, no. 14, pp. 2815–2819, 2002.
- [8] C. Kormann, D. W. Bahnemann, and M. R. Hoffmann, "Environmental photochemistry: is iron oxide (hematite) an active photocatalyst? A comparative study: α -Fe₂O₃, ZnO, TiO₂," *Journal of Photochemistry and Photobiology A*, vol. 48, no. 1, pp. 161–169, 1989.
- [9] F. Peng, H. Wang, H. Yu, and S. Chen, "Preparation of aluminum foil-supported nano-sized ZnO thin films and its photocatalytic degradation to phenol under visible light irradiation," *Materials Research Bulletin*, vol. 41, no. 11, pp. 2123–2129, 2006.
- [10] D. Li and H. Haneda, "Morphologies of zinc oxide particles and their effects on photocatalysis," *Chemosphere*, vol. 51, no. 2, pp. 129–137, 2003.
- [11] C. Hariharan, "Photocatalytic degradation of organic contaminants in water by ZnO nanoparticles," *Applied Catalysis A*, vol. 304, pp. 55–61, 2006.
- [12] M. Romero, J. Blanco, B. Sánchez et al., "Solar photocatalytic degradation of water and air pollutants: challenges and perspectives," *Solar Energy*, vol. 66, no. 2, pp. 169–182, 1999.
- [13] Y. Zheng, L. Zheng, Y. Zhan, X. Lin, Q. Zheng, and K. Wei, "Ag/ZnO heterostructure nanocrystals: synthesis, characterization, and photocatalysis," *Inorganic Chemistry*, vol. 46, no. 17, pp. 6980–6986, 2007.
- [14] L.-C. Chen, Y.-J. Tu, Y.-S. Wang, R.-S. Kan, and C.-M. Huang, "Characterization and photoreactivity of N-, S-, and C-doped ZnO under UV and visible light illumination," *Journal of Photochemistry and Photobiology A*, vol. 199, no. 2-3, pp. 170–178, 2008.
- [15] J. Liqiang, W. Baiqi, X. Baifu et al., "Investigations on the surface modification of ZnO nanoparticle photocatalyst by depositing Pd," *Journal of Solid State Chemistry*, vol. 177, no. 11, pp. 4221–4227, 2004.
- [16] W. Lu, S. Gao, and J. Wang, "One-pot synthesis of Ag/ZnO self-assembled 3D hollow microspheres with enhanced photocatalytic performance," *Journal of Physical Chemistry C*, vol. 112, no. 43, pp. 16792–16800, 2008.
- [17] X. Qiu, G. Li, X. Sun, L. Li, and X. Fu, "Doping effects of Co²⁺ ions on ZnO nanorods and their photocatalytic properties," *Nanotechnology*, vol. 19, no. 21, Article ID 215703, 8 pages, 2008.
- [18] X. Qiu, L. Li, J. Zheng, J. Liu, X. Sun, and G. Li, "Origin of the enhanced photocatalytic activities of semiconductors: a case study of ZnO doped with Mg²⁺," *Journal of Physical Chemistry C*, vol. 112, no. 32, pp. 12242–12248, 2008.
- [19] J. Lu, Q. Zhang, J. Wang, F. Saito, and M. Uchida, "Synthesis of N-Doped ZnO by grinding and subsequent heating ZnO-urea mixture," *Powder Technology*, vol. 162, no. 1, pp. 33–37, 2006.
- [20] M. L. Zhang, T. C. An, X. H. Hu, C. Wang, G. Y. Sheng, and J. M. Fu, "Preparation and photocatalytic properties of a nanometer ZnO-SnO₂ coupled Oxide," *Applied Catalysis A*, vol. 260, no. 2, pp. 215–222, 2004.
- [21] R. S. Mane, W. J. Lee, H. M. Pathan, and S. H. Han, "Nanocrystalline TiO₂/ZnO thin films: fabrication and application to dye-sensitized solar cells," *Journal of Physical Chemistry B*, vol. 109, no. 51, pp. 24254–24259, 2005.
- [22] D. Li and H. Haneda, "Synthesis of nitrogen-containing ZnO powders by spray pyrolysis and their visible-light photocatalysis in gas-phase acetaldehyde decomposition," *Journal of Photochemistry and Photobiology A*, vol. 155, no. 1-3, pp. 171–178, 2003.
- [23] M. Muruganandham and Y. Kusumoto, "Synthesis of N, C co-doped hierarchical porous microsphere ZnS as a visible light-responsive photocatalyst," *Journal of Physical Chemistry C*, vol. 113, no. 36, pp. 16144–16150, 2009.
- [24] S. S. Shinde, C. H. Bhosale, and K. Y. Rajpure, "Photocatalytic degradation of toluene using sprayed N-doped ZnO thin films in aqueous suspension," *Journal of Photochemistry and Photobiology B*, vol. 113, pp. 70–77, 2012.
- [25] C. Chandrinou, N. Boukos, C. Stogios, and A. Travlos, "PL study of oxygen defect formation in ZnO nanorods," *Microelectronics Journal*, vol. 40, no. 2, pp. 296–298, 2009.
- [26] G. R. Li, C. R. Dawa, Q. Bu et al., "Electrochemical self-assembly of ZnO nanoporous structures," *Journal of Physical Chemistry C*, vol. 111, no. 5, pp. 1919–1923, 2007.
- [27] C. S. Gopinath, S. G. Hegde, A. V. Ramaswamy, and S. Mahapatra, "Photoemission studies of polymorphic CaCO₃ materials," *Materials Research Bulletin*, vol. 37, no. 7, pp. 1323–1332, 2002.
- [28] H. Q. Sun, Y. Bai, Y. P. Cheng, W. Q. Jin, and N. P. Xu, "Preparation and characterization of visible-light-driven carbon-sulfur-codoped TiO₂ photocatalysts," *Industrial & Engineering Chemistry Research*, vol. 45, no. 14, pp. 4971–4976, 2006.
- [29] E. Papirer, R. Lacroix, J. B. Donnet, G. Nansé, and P. Fioux, "XPS study of the halogenation of carbon black—part 2. Chlorination," *Carbon*, vol. 33, no. 1, pp. 63–72, 1995.
- [30] S. Cho, J. W. Jang, J. S. Lee, and K. H. Lee, "Carbon-doped ZnO nanostructures synthesized using vitamin C for visible light photocatalysis," *CrystEngComm*, vol. 12, no. 11, pp. 3929–3935, 2010.
- [31] J. G. Ma, Y. C. Liu, R. Mu et al., "Method of control of nitrogen content in ZnO films: structural and photoluminescence properties," *Journal of Vacuum Science & Technology B*, vol. 22, no. 1, pp. 94–98, 2004.
- [32] X. Wang, J. C. Yu, Y. Chen, L. Wu, and X. Fu, "ZrO₂-modified mesoporous nanocrystalline TiO_{2-x}N_x as efficient visible light photocatalysts," *Environmental Science and Technology*, vol. 40, no. 7, pp. 2369–2374, 2006.

- [33] Y. F. Mei, R. K. Y. Fu, G. G. Siu et al., "Nitrogen binding behavior in ZnO films with time-resolved cathodoluminescence," *Applied Surface Science*, vol. 252, no. 23, pp. 8131–8134, 2006.
- [34] S. Sato, R. Nakamura, and S. Abe, "Visible-light sensitization of TiO₂ photocatalysts by wet-method N doping," *Applied Catalysis A*, vol. 284, no. 1-2, pp. 131–137, 2005.
- [35] R. Asahi, T. Morikawa, T. Ohwaki, K. Aoki, and Y. Taga, "Visible-light photocatalysis in nitrogen-doped titanium oxides," *Science*, vol. 293, no. 5528, pp. 269–271, 2001.
- [36] J. C. Yu, W. Ho, J. Yu, H. Yip, K. W. Po, and J. Zhao, "Efficient visible-light-induced photocatalytic disinfection on sulfur-doped nanocrystalline titania," *Environmental Science and Technology*, vol. 39, no. 4, pp. 1175–1179, 2005.
- [37] T. Ohno, M. Akiyoshi, T. Umebayashi, K. Asai, T. Mitsui, and M. Matsumura, "Preparation of S-doped TiO₂ photocatalysts and their photocatalytic activities under visible light," *Applied Catalysis A*, vol. 265, no. 1, pp. 115–121, 2004.
- [38] T. Ohno, T. Tsubota, Y. Nakamura, and K. Sayama, "Preparation of S, C cation-codoped SrTiO₃ and its photocatalytic activity under visible light," *Applied Catalysis A*, vol. 288, no. 1-2, pp. 74–79, 2005.
- [39] A. Zaleska, P. Górska, J. W. Sobczak, and J. Hupka, "Thioacetamide and thiourea impact on visible light activity of TiO₂," *Applied Catalysis B*, vol. 76, no. 1-2, pp. 1–8, 2007.
- [40] S. Anandan, A. Vinu, K. L. P. S. Lovely et al., "Photocatalytic activity of La-doped ZnO for the degradation of monocrotophos in aqueous suspension," *Journal of Molecular Catalysis A*, vol. 266, no. 1-2, pp. 149–157, 2007.
- [41] X. H. Wang, S. Liu, P. Chang, and Y. Tang, "Influence of S incorporation on the luminescence property of ZnO nanowires by electrochemical deposition," *Physics Letters A*, vol. 372, no. 16, pp. 2900–2903, 2008.
- [42] B. Stypula and J. Stoch, "The characterization of passive films on chromium electrodes by XPS," *Corrosion Science*, vol. 36, no. 12, pp. 2159–2167, 1994.
- [43] C. Shifu, Z. Sujuan, L. Wei, and Z. Wei, "Preparation and activity evaluation of p–n junction photocatalyst NiO/TiO₂," *Journal of Hazardous Materials*, vol. 155, no. 1-2, pp. 320–326, 2008.
- [44] C. Shifu, Z. Wei, Z. Sujuan, and L. Wei, "Preparation, characterization and photocatalytic activity of N-containing ZnO powder," *Chemical Engineering Journal*, vol. 148, no. 2-3, pp. 263–269, 2009.
- [45] J. W. Jung, H. C. Lee, and J. S. Wang, "A study on the double insulating layer for HgCdTe MIS structure," *Thin Solid Films*, vol. 290-291, pp. 18–22, 1996.



Hindawi

Submit your manuscripts at
<http://www.hindawi.com>

